nature publishing group

Effects of nonocclusive mesenteric hypertension on intestinal function: implications for gastroschisis-related intestinal dysfunction

Shinil K. Shah[1], Kevin R. Aroom[2], Peter A. Walker[1], Hasen Xue[2], Fernando Jimenez[2], Brijesh S. Gill[1], Charles S. Cox Jr[2] and Stacey D. Moore-Olufemi[2]

INTRODUCTION: Infants with gastroschisis (GS) have significant morbidity from dysmotility, feeding intolerance, and are at increased risk of developing intestinal failure. Although the molecular mechanisms regulating GS-related intestinal dysfunction (GRID) are largely unknown, we hypothesized that mechanical constriction (nonocclusive mesenteric hypertension (NMH)) from the abdominal wall defect acts as a stimulus for GRID. The purpose of this study was to determine the effect of NMH on intestinal function and inflammation.

METHODS: Neonatal rats had placement of a silastic disk to the base of the mesentery (NMH) or no disk placement (Sham). At 24 and 72 h, mesenteric venous pressures (MVPs), intestinal transit, electric impedance, permeability, length, and tissue water content were measured.

RESULTS: After placement of the silastic disk, there was a significant increase in MVP at both time points. There was also decreased intestinal transit. As compared to Sham animals, NMH animals had significant changes in bowel impedance without an increase in tissue water, suggesting significant intestinal remodeling. NMH rats had significantly increased smooth-muscle thickness and loss of intestinal length as compared with Sham rats.

DISCUSSION: NMH may be an initiating factor for GRID. Measurement of MVP and/or bowel impedance may be a way to assess severity and monitor progression and/or resolution of GRID.

Gastroschisis (GS) is the most common congenital abdominal wall defect and the most common reason for intestinal transplantation affecting infants today. The incidence of GS is increasing worldwide and occurs in ~1 in every 2,000–4,000 live births in the United States. The economic burden of GS-related intestinal dysfunction (GRID) is significant, with an estimated yearly cost of $128,414,475 in the United States alone (2004 dollars (1–4)). The intestine is particularly susceptible to injury, resulting in edema, ileus, and failure of intestinal defense mechanisms. These factors are commonly seen in infants affected with GS and can increase morbidity and length of hospital stay. Although the molecular mechanisms regulating the intestinal dysfunction associated with GS are largely unknown, surgical models of GS have shown that venous constriction causes lymphatic and venous dilation, smooth-muscle thickening, and focal mucosal blunting, contributing to intestinal dysfunction (5,6).

Current limitations involved in advancing our understanding of GRID involve use of fetal animal models with poor postnatal survival and high maintenance costs (7,8). It is well known that GS results in intestinal failure; however, therapies to prevent GRID are completely lacking because of the limited knowledge of the intestinal response to GS injury. Two dominant risk factors for the development of GRID have been identified in humans and animal models: (i) the GS abdominal wall defect and (ii) intestinal exposure to amniotic fluid (AF). These risk factors contribute to smooth-muscle thickening and shortened intestinal length in the intestine. What is not known is if re-creating the local environment can produce similar changes in the intestine outside the antenatal period. The purpose of this study was to model the abdominal wall defect and exposure to AF to further delineate the pathophysiology of GRID. We hypothesized that mechanical constriction of the intestinal mesentery will produce a similar pattern of GS-related intestinal injury in postnatal animals, and that AF further contributes to this process.

RESULTS

Figure 1 demonstrates that placement of the silastic disk caused a significant elevation in the MVP at 24 and 72 h (nonocclusive mesenteric hypertension (NMH)-24: 7.3 ± 0.2 mm Hg and NMH-72: 9.0 ± 0.8 mm Hg) as compared with Sham animals (Sham: 4.0 ± 0.4 mm Hg).

As shown in **Figure 2**, the intestine was more permeable to fluorescein isothiocyanate–conjugated dextran in the NMH animals at 24 and 72 h (NMH-24: 0.3 ± 0.1 and NMH-72: 0.5 ± 0.2) as compared with Sham animals (Sham-24: 0.09 ± 0.0 and Sham-72: 0.14 ± 0.0).

As shown in **Figure 3** using our impedance analyzer system, the impedance curves are shifted to the left in the NMH

[1]Department of Surgery, University of Texas Medical School at Houston, Houston, Texas; [2]Department of Pediatric Surgery, University of Texas Medical School at Houston, Houston, Texas. Correspondence: Stacey D. Moore-Olufemi (Stacey.D.Moore-Olufemi@uth.tmc.edu)

Received 27 July 2011; accepted 23 January 2012; advance online publication 4 April 2012. doi:10.1038/pr.2012.20

animals at 24 and 72 h as compared with the Sham animals, indicating a significant decrease in tissue impedance due to reductions in both resistance and reactance.

As shown in **Figure 4**, contractility was significantly decreased in NMH animals at 24 h (NMH-24: 3.1 ± 0.7) as compared with Sham animals (Sham-24: 8.2 ± 2.0). After carbachol stimulation, contractility improved in the NMH animals (NMH-24: 8.4 ± 2.1), but there was no difference in Sham animals (Sham-24: 12 ± 2.6).

The data depicted in **Figure 5** demonstrate that intestinal transit, reported as mean geometric center (MGC), was significantly impaired in the NMH animals at 24 and 72 h (NMH-24: 5.0 ± 0.5 MGC and NMH-72: 6.1 ± 0.3 MGC) as compared with Sham animals (Sham-24: 6.0 ± 0.4 MGC and Sham-72: 8.0 ± 0.1 MGC). The addition of AF also significantly impaired intestinal transit in the NMH + AF animals at 24 and 72 h (NMH + AF-24: 4.0 ± 0.4 MGC and NMH + AF-72: 5.6 ± 0.4 MGC) as compared with Sham animals at both time points.

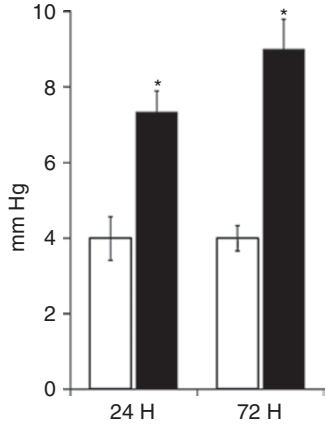

Figure 1. Mesenteric venous pressure. Mesenteric venous pressure (mm Hg) results are presented as means ± SEM. *$P < 0.05$ using Student's *t*-test. $n = 5–6$. Sham, open bars; NMH, filled bars. NMH, nonocclusive mesenteric hypertension.

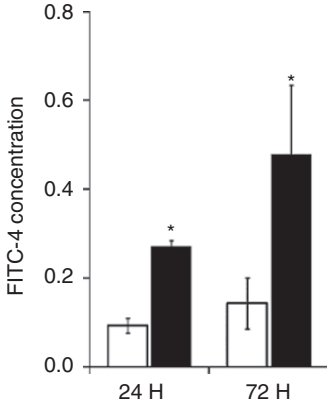

Figure 2. Intestinal permeability. Intestinal permeability to FITC (FITC-4) is presented as mean ± SEM. *$P < 0.05$ using Student's *t*-test. $n = 5–6$. Sham, open bars; NMH, filled bars. FITC, fluorescein isothiocyanate–conjugated dextran; NMH, nonocclusive mesenteric hypertension.

Representative hematoxylin and eosin-stained sections of ileum from Sham, Sham + AF, NMH, and NMH + AF animals are depicted in **Figure 6a,b**. The smooth-muscle layer in NMH animals was significantly thicker (NMH-24: 90 ±

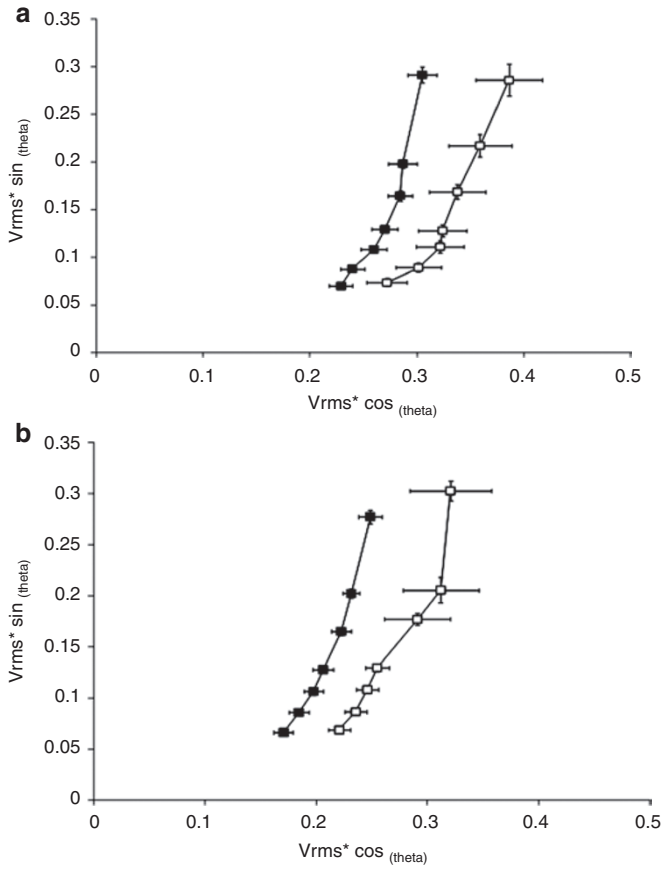

Figure 3. Intestinal impedance. (**a**) 24 h and (**b**) 72 h. Impedance results are presented as means ± SEM. $n = 5–6$. Impedance is plotted on the *x*-axis and *y*-axis according to resistance and reactance, respectively. Vrms = root mean square of the voltage signal. A decrease in tissue reactance is due to an increase in tissue capacitance across the tissue. Sham, open squares; NMH, filled squares. NMH, nonocclusive mesenteric hypertension.

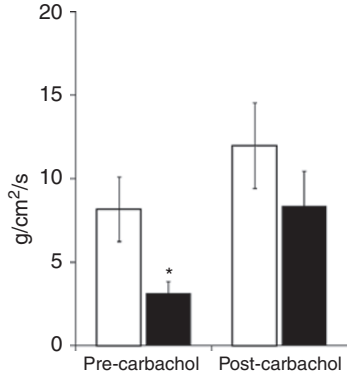

Figure 4. Intestinal contractility. Basal intestinal contractile strength (g/cm²/s) is significantly reduced in NMH prior to carbachol stimulation. Contractile strength is presented as mean ± SEM. *$P < 0.05$ using Student's *t*-test. $n = 5–6$. Sham, open bars; NMH, filled bars. NMH, nonocclusive mesenteric hypertension.

8 μm and NMH-72: 102 ± 12 μm) at 24 and 72 h as compared with Sham animals (Sham-24: 56 ± 3 μm and Sham-72: 68 ± 6 μm, Figure 6c). Exposure to AF resulted in a thicker smooth-muscle layer in Sham + AF and NMH + AF, but there was no difference between the two groups.

Figure 7 shows that there was no difference in wet:dry ratios among the groups at 24 h. By 72 h, NMH animals exposed to AF (4.6 ± 0.2) had a significant increase in tissue water as compared with Sham animals exposed to AF.

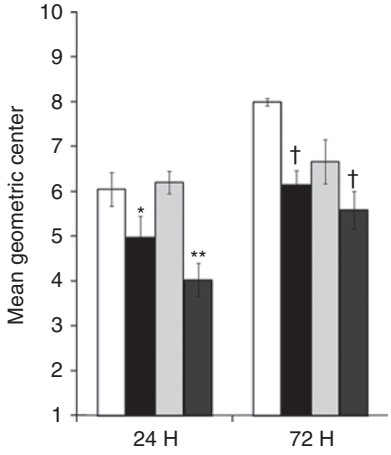

Figure 5. Intestinal transit. The mean geometric center (MGC) of tracer is presented as mean ± SEM. *P < 0.05 vs. Sham at 24 h; **P < 0.05 vs. Sham and Sham + AF at 24 h; †P < 0.05 vs. Sham at 72 h using two-way ANOVA. n = 5–6. Sham, open bars; NMH, black bars; Sham + AF, light gray bars; NMH + AF, dark gray bars. AF, amniotic fluid; NMH, nonocclusive mesenteric hypertension.

The data depicted in Figure 8 demonstrate that there was a significant decrease in intestinal length in the NMH animals at 24 and 72 h (NMH-24: 62 ± 2 cm and NMH-72: 61 ± 3 cm) as compared with Sham animals (Sham-24: 80 ± 2 cm and Sham-72: 76 ± 2 cm). Exposure to AF was associated with a significant decrease in intestinal length in the NMH animals at 24 h (NMH + AF-24: 67 ± 2 cm) as compared with Sham animals (Sham-24: 61 ± 1 cm). However, by 72 h, exposure to AF decreased intestinal length in the Sham and NMH animals exposed to AF.

There were no differences among the groups in the plasma cytokine levels at 24 and 72 h (data not shown). The data depicted in Figure 9a,b demonstrate that there were increased tissue levels of the proinflammatory cytokines tumor necrosis factor-α, interferon-γ, and interleukin (IL)-6 in the NMH animals with and without exposure to AF at 24 and 72 h as compared with Sham animals. Figure 9c also shows increased levels of the proinflammatory mediator, osteopontin in the NMH animals with and without exposure to AF as compared with Sham animals.

DISCUSSION

Our group is focused on understanding the pathophysiology of GRID and the implications of mechanical constriction from the abdominal wall defect and exposure to AF for intestinal dysfunction. Although studies investigating GS intestinal injury

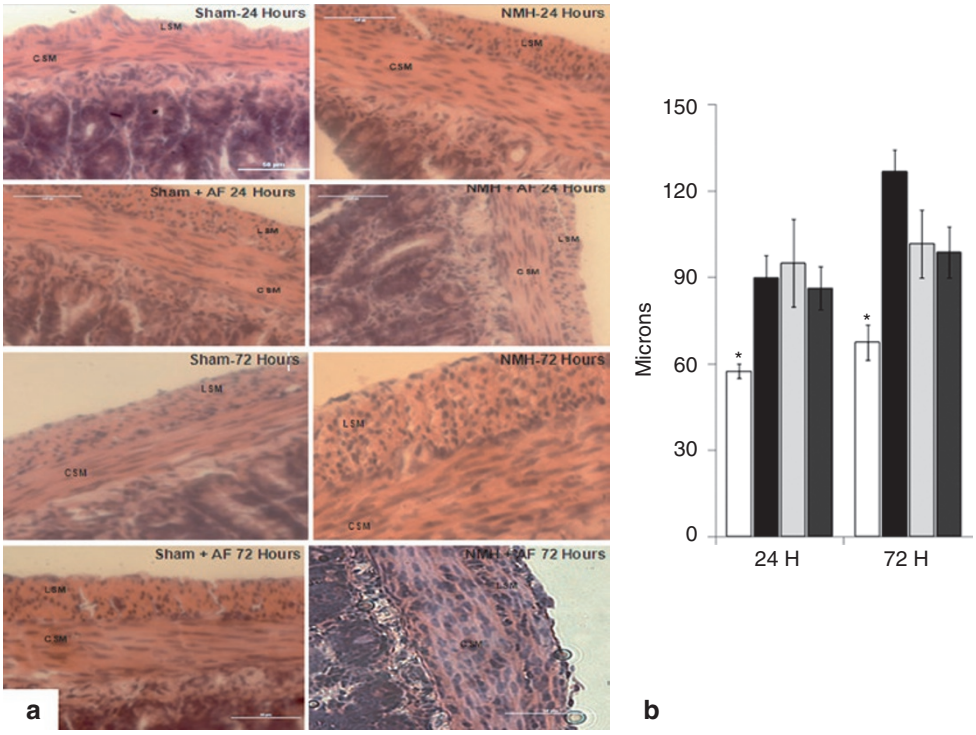

Figure 6. Smooth-muscle histology. (**a**) Formalin-fixed, paraffin-embedded sections of ileum stained with hematoxylin and eosin. Original magnification ×60. (**b**) Smooth-muscle thickness was measured in microns and expressed as mean ± SEM. *P < 0.05 vs. all groups at 24 and 72 h using two-way ANOVA. n = 3–4 for each group. Sham, open bars; NMH, black bars; Sham + AF, light gray bars; NMH + AF, dark gray bars. AF, amniotic fluid; CSM, circular smooth muscle; LSM, longitudinal smooth muscle; NMH, nonocclusive mesenteric hypertension.

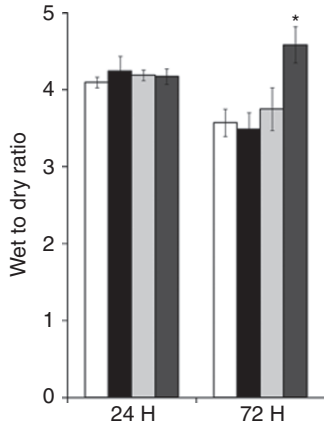

Figure 7. Intestinal edema. Tissue water weight was calculated as a wet weight:dry weight ratio and expressed as mean ± SEM. *P < 0.05 vs. all groups at 72 h using two-way ANOVA. n = 5–6 for each group. Sham, open bars; NMH, black bars; Sham + AF, light gray bars; NMH + AF, dark gray bars. AF, amniotic fluid; NMH, nonocclusive mesenteric hypertension.

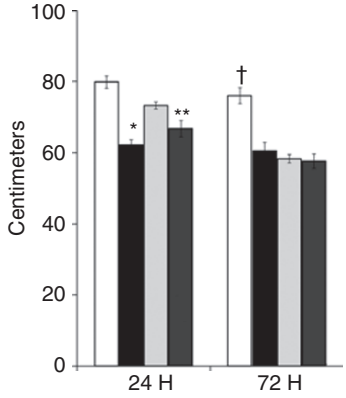

Figure 8. Intestinal length. Intestinal length was measured in centimeters and expressed as mean ± SEM. *P < 0.05 vs. Sham and Sham + AF at 24 h; **P < 0.05 vs. Sham at 24 h; †P < 0.05 vs. all groups at 72 h using two-way ANOVA. n = 5–6 for each group. Sham, open bars; NMH, black bars; Sham + AF, light gray bars; NMH + AF, dark gray bars. AF, amniotic fluid; NMH, nonocclusive mesenteric hypertension.

have been conducted in fetal animal models, we have successfully reconstructed the local environment of the abdominal wall defect and exposure to AF in a postnatal animal, demonstrating a similar intestinal injury pattern to that seen in human and fetal subjects (5–6,9–12). In the results presented, we demonstrated that mechanical constriction of the intestinal mesentery was associated with decreased intestinal motility, contractility, bioimpedance, and length, and increased MVP, intestinal permeability, smooth-muscle thickness, and a local inflammatory response. Exposure to AF was also found to decrease intestinal motility and length and increase smooth-muscle thickness and local inflammation.

Previous studies have placed emphasis on the developmental components of the abdominal wall defect, as well as exposure of the intestine to toxic substances on GS-related intestinal injury, but there has been little information regarding the impact of mesenteric venous hypertension on gut dysfunction (4–7). Our results provide new evidence that NMH delays intestinal transit, decreases contractility, and increases mucosal permeability. Our group has demonstrated that acute (<6 h) mesenteric venous hypertension along with fluid resuscitation delays intestinal transit and increases mucosal permeability (13). Our previous study also showed that fluid resuscitation alone generated gut edema, but fluid alone was not enough to produce alterations in gut function. Our results did not produce comparable levels of edema seen in that study; however, in the setting of NMH, we were able to produce the same level of gut dysfunction. In a previous study we have also demonstrated that intestinal contractility can be used as a surrogate marker of transit (14). Our results showed that NMH was associated with a significant decrease in contractility, which was reflective of our transit experiments. Only the addition of carbachol resulted in a slight improvement of contractile dysfunction associated with NMH. This suggests that there is a primary smooth-muscle dysfunction that is responsible for impaired transit and contractile function in the gut and is a subject of potential future investigation.

Smooth-muscle compliance and plasticity are important properties of the intestine and play an important role in the initiation

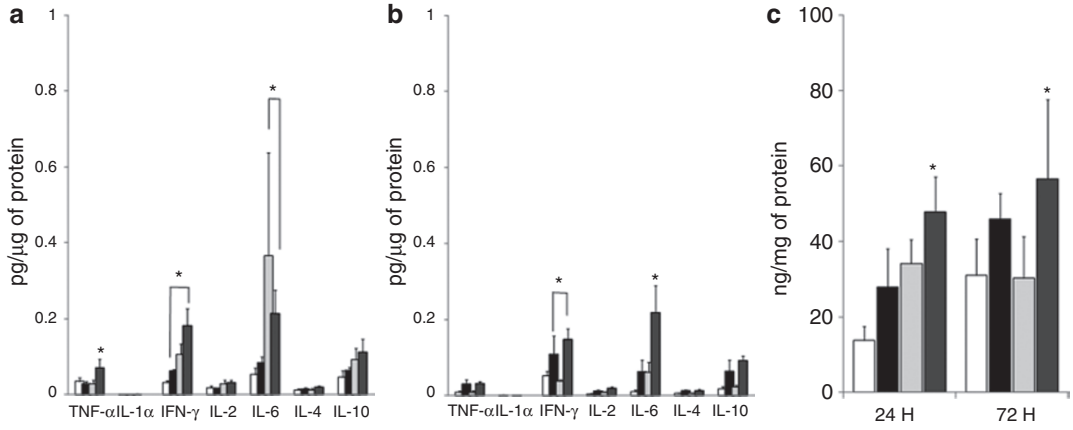

Figure 9. Inflammation. (**a**) 24 h, (**b**) 72 h, and (**c**) OPN. Tissue cytokine levels were measured and normalized to total plasma protein concentrations and expressed as means ± SEM. *P < 0.05 vs. all groups at 24 and 72 h using two-way ANOVA. n = 4–5 for each group. Sham, open bars; NMH, black bars; Sham + AF, light gray bars; NMH + AF, dark gray bars. AF, amniotic fluid; IFN, interferon; IL, interleukin; NMH, nonocclusive mesenteric hypertension; OPN, osteopontin; TNF, tumor necrosis factor.

and maintenance of intestinal motility (12). Electrical impedance is a useful tool for measuring the complexities of tissue resistance and capacitance. Previous studies have demonstrated that tissue capacitance increase as tissue water concentrations increase (13). Impedance analysis has been utilized extensively in cardiac muscle research to predict the extent of tissue injury associated with ischemia/reperfusion. These studies demonstrated that the major determinates of myocardial impedance included changes in extracellular and intracellular resistance, gap junction conductance, and cell membrane capacitance (15–18). In our study, NMH increased the tissue capacitance and water content of the small intestine and increased smooth-muscle thickness. Impedance analysis may provide further insight into GRID; further studies need to be conducted to determine the effects of NMH on smooth-muscle function.

It has been well documented that intestinal inflammation in various injury models has deleterious effects on intestinal function (19). NMH was associated with an increase in proinflammatory mediators such as tumor necrosis factor-α, interferon-γ, and IL-6; this may perpetuate the effects of delayed intestinal transit in addition to elevated MVP. Osteopontin, another proinflammatory cytokine that has recently emerged as a key factor in this airway and vascular smooth-muscle dysfunction was elevated with NMH (20,21). It has yet to be determined whether osteopontin is a key player in the intestinal dysfunction in our model. In a model of surgical manipulation, local infiltration of macrophages and neutrophils was linked to the intestinal ileus (22,23). Interferon-γ, IL-6, and osteopontin, all products of macrophages, were increased in the intestine at 24 and 72 h, and this same infiltration of macrophages may potentially play a role in prolonged intestinal dysfunction in our model.

Significant morbidity continues to exist as a result of intestinal failure in patients with GS. Although estimates of normal intestinal length exist for preterm and term infants (24), these normative data have not been adequately documented in infants with GS. Our data confirm previous reports from other animal models (7,25) that intestinal length is markedly decreased.

AF has been shown to have increased levels of inflammatory cells and cytokines, and prolonged exposure to AF has long been thought to initiate serosal fibrosis ("peel") and intestinal injury (26–27). More recent human data suggest that intestinal exposure to AF does not result in serosal fibrosis; however, the intestinal dysfunction persists (28). Although "peel" formation in our study was not apparent, intestines exposed to AF demonstrated a similar injury pattern to that of the NMH animals. These changes have been well documented in other fetal models of GS (5,6) and represent a pattern that occurs in intestinal smooth muscle as a result of environmental and mechanical stimuli. This "smooth-muscle" response to various environmental and mechanical stimuli has been well characterized in the vascular smooth-muscle system. Vascular smooth muscle typically responds by increasing its synthetic phenotypic behavior (29,30). Airway smooth-muscle cells also respond in a similar fashion to various stimuli with a synthetic phenotypic response (31–33). Although in this report we do not measure the intestinal smooth-muscle synthetic response, our data suggest that NMH triggers a smooth-muscle response that is further exacerbated by exposure to AF.

One limitation of this study is that this represents only a surrogate model to study human GS. Although our postnatal model leaves out the developmental aspects of the intestine, we believe that the pathophysiology resulting in the intestinal injury from GS results from chronic elevation of MVP, triggering an inflammatory response in the intestinal smooth muscle. This injury is further exacerbated by intestinal exposure to AF.

In conclusion, we have shown that NMH produced an intestinal injury pattern similar to the current animal models of GS. AF further exacerbates this injury. Our model provides an opportunity to explore some of the basic mechanisms driving intestinal dysfunction and will allow us to conduct further studies into the pathophysiology of GRID.

METHODS

The University of Texas Animal Welfare Committee approved all procedures according to the National Institutes of Health *Guide for the Care and Use of Laboratory Animals.*

Male neonatal Sprague-Dawley rats weighing between 40 and 60 g (Harlan Labs, Indianapolis, IN) were fasted 10–12 h prior to NMH protocol surgery and given free access to water. NMH Protocol: Under general anesthesia with isoflurane using aseptic technique, a midline laparotomy incision was made and the small intestine was exteriorized for placement of a 3/4-inch silastic disk (Allied Biomedical, Ventura, CA) with a 1/4-inch internal diameter nonobstructing defect applied to the base of the mesentery to include the entire length of the bowel from the duodenum to cecum (NMH) or no disk placement (Sham) and then the small intestine was returned to the peritoneal cavity and the midline incision was closed. The rats were then returned to the animal facility after recovery and kept under 12-h light and dark cycles and given ad libitum standard rat chow and free access to water until they were killed.

A separate group of rats had a mouse port-a-catheter (Braintree Scientific, Braintree, MA) introduced into the peritoneal cavity. The silastic catheter portion of the port-a-catheter was tunneled through the subcutaneous tissue and passed through the musculature of the right abdominal wall, and the port-a-catheter hub was secured to the back of the neck with a 5-0 Vicryl suture using a separate interscapular incision. The port was accessed daily for injection of 4 ml of AF obtained from pregnant female rats (Bioreclamation, Westbury, NY).

Experimental Design

In the first experiment (**Figure 10a**), rats were randomized to the following groups: Sham and NMH and further subdivided into 24- and 72-h time points to determine the effects of NMH on intestinal transit, contractility and permeability, smooth-muscle histology, intestinal length, tissue water weight, and local inflammation. $N = 5–6$/group.

In the second experiment (**Figure 10b**), rats were randomized to the following groups: Sham + AF and NMH + AF and further subdivided into 24- and 72-h time points to determine the effects of AF on intestinal transit, smooth-muscle histology, intestinal length, tissue water weight, and local inflammation. $N = 5–6$/group.

A separate set of rats underwent cannulation of a branch of the superior mesenteric vein for determination of baseline MVPs. To evaluate the effects of immediate placement of the NMH defect, a branch of the superior mesenteric vein was cannulated immediately after placement to evaluate the degree of acute NMH. All measurements were taken using a pressure transducer connected to a monitor/terminal (78534B; Hewlett Packard, Palo Alto, CA).

In vivo intestinal permeability was measured by methods adapted from Wang *et al.* (34). By oral gavage, rats were administered

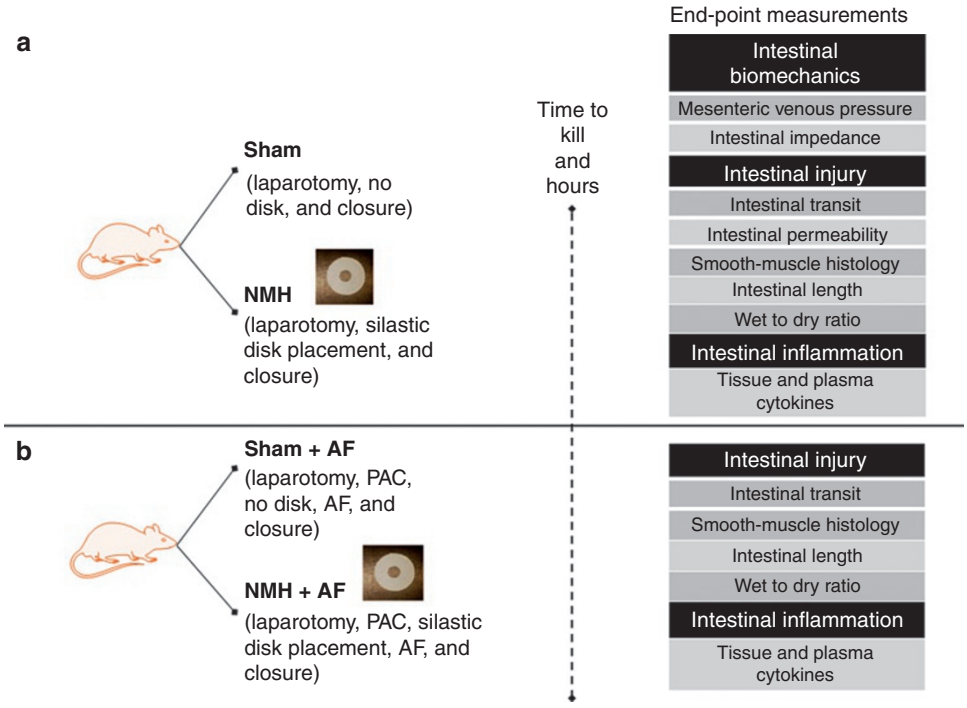

Figure 10. Schematic of nonocclusive mesenteric hypertension model. (**a**) Experiment 1 determined the effects of nonocclusive mesenteric hypertension on intestinal injury and inflammation. (**b**) Experiment 2 determined the effects of AF on intestinal injury and inflammation. AF, amniotic fluid; NMH, nonocclusive mesenteric hypertension; PAC, port-a-catheter.

20 ml/kg of a 22 mg/ml solution of fluorescein isothiocyanate–conjugated dextran (molecular weight 4.4 kDa; Sigma, St. Louis, MO). Six hours after administration, plasma was collected by cardiac puncture and assessed fluorometrically for concentration of fluorescein isothiocyanate–conjugated dextran.

Electrical impedance was measured across a spectrum of frequencies using a customized impedance analyzer system, as described by Radhakrishnan *et al.* (35). At 24 and 72 h, the animals were placed under general anesthesia again and the laparotomy incisions were reopened. Four small electrodes of gold wire were placed on the serosal side of the distal ileum, 5–7 cm from the ileocecal valve. Using the bowel in our circuit, the impedance analyzer system was then used to measure impedance at frequencies from 100 Hz to 100 kHz.

Intestinal contractility was measured by methods previously performed by our laboratory (14). In brief, full-thickness intestinal strips were mounted in organ baths filled with Krebs-Ringer solution. Isometric force was monitored by an external force displacement transducer (Quantametrics, Newtown, PA) connected to a PowerLab data acquisition system (AD Instruments, Colorado Springs, CO). Each strip was stretched to optimal length, then allowed to equilibrate for at least 30 min prior to any measurements. After equilibration, 30 min of basal contractile activity data were recorded. The intestinal strips were then treated with 10^{-6} mol/l carbachol and contractile activity data were recorded for 5 min.

Intestinal transit was measured according to previously published methods and determined by distribution of a nonabsorbable 70 kDa fluorescein isothiocyanate–labeled dextran (FD70 (36)). Briefly, 200 µl of 2.5 mg/ml solution (dissolved in distilled water) was administered by oral gavage. After 60 min, the supernatant of the resultant samples was collected and assessed fluorometrically for concentration of 70 kDa fluorescein isothiocyanate–labeled dextran. Transit was evaluated by calculating the geometric center of distribution of 70 kDa fluorescein isothiocyanate–labeled dextran (Σ (fluorescent signal per segment (percent) × segment number)/100).

Three centimeters of distal ileum was removed at 24 and 72 h and stored in 10% formalin until processing. The tissues were embedded in paraffin blocks, sectioned, placed on glass microscope slides and stained with hematoxylin and eosin. Smooth-muscle histology: Smooth-muscle morphometrics were examined by light microscopy at ×60 by a pathologist blinded as to group. The circular and longitudinal muscle thickness were expressed in microns and presented as total muscle thickness (n = 3–4/group). All measurements were taken on static images utilizing NIS-Elements software (AR 3.0; Nikon Instruments, Melville, NY).

The small intestine from the duodenum to the ileum at the ileocecal valve was harvested at 24 and 72 h to determine the tissue water content. Wet weight was determined prior to placing tissue in an oven set to 60 °C for 3 d, and dry weights were measured and used to determine tissue water content using the following formula: ((wet weight − dry weight)/dry weight), as previously described by our group (13).

The small intestine from the duodenum to the ileum at the ileocecal valve was harvested at 24 and 72 h to determine the intestinal length. The intestinal length was measured by placing the entire length of the intestine in a straight line against a standardized tape marked in centimeters for all intestine harvested from each animal.

Cytokines were detected in the plasma and whole-tissue cell lysates were detected using the Bio-Plex cytokine assay system (Bio-Rad Laboratories, Hercules, CA) and Osteopontin (OPN) Enzyme Immunoassay kit (Stressgen, Ann Arbor, MI). Concentrations of IL-1α, IL-2, IL-4, IL-6, IL-10, interferon-γ, and tumor necrosis factor-α were measured using a multiplex bead array (Rat 9-Plex; Bio-Rad Laboratories, Hercules, CA). The assay was performed per the manufacturer's instructions, and the details have been previously published by our group and others (37,38). All samples were run in duplicate.

Statistical Analysis

All data are expressed as means ± SEM using a commercial statistical software program (NCSS, Kaysville, UT). Statistical significance was determined using either a two-way ANOVA followed by a Tukey–Kramer multiple comparison test or Student's t-test to compare effects of NMH with and without the effects of AF. A P value <0.05 was considered significant.

STATEMENT OF FINANCIAL SUPPORT
This study was supported by National Institutes of Health grant T32 GM 0879201 and Robert Woods Johnson Foundation grant 68517.

REFERENCES

1. Alvarez SM, Burd RS. Increasing prevalence of gastroschisis repairs in the United States: 1996-2003. J Pediatr Surg 2007;42:943–6.
2. Lao OB, Larison C, Garrison MM, Waldhausen JH, Goldin AB. Outcomes in neonates with gastroschisis in U.S. children's hospitals. Am J Perinatol 2010;27:97–101.
3. Centers for Disease Control and Prevention (CDC). Hospital stays, hospital charges, and in-hospital deaths among infants with selected birth defects—United States, 2003. MMWR Morb Mortal Wkly Rep 2007;56(2):25–9.
4. Spencer AU, Kovacevich D, McKinney-Barnett M, et al. Pediatric short-bowel syndrome: the cost of comprehensive care. Am J Clin Nutr 2008;88:1552–9.
5. Langer JC, Longaker MT, Crombleholme TM, et al. Etiology of intestinal damage in gastroschisis. I: Effects of amniotic fluid exposure and bowel constriction in a fetal lamb model. J Pediatr Surg 1989;24:992–7.
6. Midrio P, Faussone-Pellegrini MS, Vannucchi MG, Flake AW. Gastroschisis in the rat model is associated with a delayed maturation of intestinal pacemaker cells and smooth muscle cells. J Pediatr Surg 2004;39:1541–7.
7. Oyachi N, Lakshmanan J, Ross MG, Atkinson JB. Fetal gastrointestinal motility in a rabbit model of gastroschisis. J Pediatr Surg 2004;39:366–70.
8. Stephenson JT, Pichakron KO, Vu L, et al. In utero repair of gastroschisis in the sheep (Ovis aries) model. J Pediatr Surg 2010;45:65–9.
9. Tibboel D, Raine P, McNee M, et al. Developmental aspects of gastroschisis. J Pediatr Surg 1986;21:865–9.
10. Tibboel D, Vermey-Keers C, Klück P, Gaillard JL, Koppenberg J, Molenaar JC. The natural history of gastroschisis during fetal life: development of the fibrous coating on the bowel loops. Teratology 1986;33:267–72.
11. Langer JC. Fetal abdominal wall defects. Semin Pediatr Surg 1993;2:121–8.
12. Spencer NJ, Smith CB, Smith TK. Role of muscle tone in peristalsis in guinea-pig small intestine. J Physiol (Lond) 2001;530(Pt 2):295–306.
13. Moore-Olufemi SD, Xue H, Attuwaybi BO, et al. Resuscitation-induced gut edema and intestinal dysfunction. J Trauma 2005;58:264–70.
14. Uray KS, Laine GA, Xue H, Allen SJ, Cox CS Jr. Intestinal edema decreases intestinal contractile activity via decreased myosin light chain phosphorylation. Crit Care Med 2006;34:2630–7.
15. Cinca J, Warren M, Carreño A, et al. Changes in myocardial electrical impedance induced by coronary artery occlusion in pigs with and without preconditioning: correlation with local ST-segment potential and ventricular arrhythmias. Circulation 1997;96:3079–86.
16. van Oosterom A, de Boer RW, van Dam RT. Intramural resistivity of cardiac tissue. Med Biol Eng Comput 1979;17:337–43.
17. Ellenby MI, Small KW, Wells RM, Hoyt DJ, Lowe JE. On-line detection of reversible myocardial ischemic injury by measurement of myocardial electrical impedance. Ann Thorac Surg 1987;44:587–97.
18. Gebhard MM, Gersing E, Brockhoff CJ, Schnabel PA, Bretschneider HJ. Impedance spectroscopy: a method for surveillance of ischemia tolerance of the heart. Thorac Cardiovasc Surg 1987;35:26–32.
19. Peuhkuri K, Vapaatalo H, Korpela R. Even low-grade inflammation impacts on small intestinal function. World J Gastroenterol 2010;16:1057–62.
20. Kurata M, Okura T, Watanabe S, Fukuoka T, Higaki J. Osteopontin and carotid atherosclerosis in patients with essential hypertension. Clin Sci 2006;111:319–24.
21. Kohan M, Breuer R, Berkman N. Osteopontin induces airway remodeling and lung fibroblast activation in a murine model of asthma. Am J Respir Cell Mol Biol 2009;41:290–6.
22. Schwarz NT, Kalff JC, Türler A, et al. Selective jejunal manipulation causes postoperative pan-enteric inflammation and dysmotility. Gastroenterology 2004;126:159–69.
23. Kalff JC, Hierholzer C, Tsukada K, Billiar TR, Bauer AJ. Hemorrhagic shock results in intestinal muscularis intercellular adhesion molecule (ICAM-1) expression, neutrophil infiltration, and smooth muscle dysfunction. Arch Orthop Trauma Surg 1999;119:89–93.
24. Touloukian RJ, Smith GJ. Normal intestinal length in preterm infants. J Pediatr Surg 1983;18:720–3.
25. Correia-Pinto J, Tavares ML, Baptista MJ, Estevão-Costa J, Flake AW, Leite-Moreira AF. A new fetal rat model of gastroschisis: development and early characterization. J Pediatr Surg 2001;36:213–6.
26. Morrison JJ, Klein N, Chitty LS, et al. Intra-amniotic inflammation in human gastroschisis: possible aetiology of postnatal bowel dysfunction. Br J Obstet Gynaecol 1998;105:1200–4.
27. Guibourdenche J, Berrebi D, Vuillard E, et al. Biochemical investigations of bowel inflammation in gastroschisis. Pediatr Res 2006;60:565–8.
28. Deans KJ, Mooney DP, Meyer MM, Shorter NA. Prolonged intestinal exposure to amniotic fluid does not result in peel formation in gastroschisis. J Pediatr Surg 1999;35:975–6.
29. Mitchell GM, McCann JJ, Rogers IW, Hickey MJ, Morrison WA, O'Brien BM. A morphological study of the long-term repair process in experimentally stretched but unruptured arteries and veins. Br J Plast Surg 1996;49:34–40.
30. Acampora KB, Nagatomi J, Langan EM III, LaBerge M. Increased synthetic phenotype behavior of smooth muscle cells in response to *in vitro* balloon angioplasty injury model. Ann Vasc Surg 2010;24:116–26.
31. Lazaar AL, Panettieri RA Jr. Airway smooth muscle: a modulator of airway remodeling in asthma. J Allergy Clin Immunol 2005;116:488–95; quiz 496.
32. Nguyen TT, Ward JP, Hirst SJ. beta1-Integrins mediate enhancement of airway smooth muscle proliferation by collagen and fibronectin. Am J Respir Crit Care Med 2005;171:217–23.
33. Hirst SJ, Martin JG, Bonacci JV, et al. Proliferative aspects of airway smooth muscle. J Allergy Clin Immunol 2004;114(Suppl 2):S2–17.
34. Wang Q, Fang CH, Hasselgren PO. Intestinal permeability is reduced and IL-10 levels are increased in septic IL-6 knockout mice. Am J Physiol Regul Integr Comp Physiol 2001;281:R1013–23.
35. Radhakrishnan RS, Shah K, Xue H, et al. Measurement of intestinal edema using an impedance analyzer circuit. J Surg Res 2007;138:106–10.
36. Miller MS, Galligan JJ, Burks TF. Accurate measurement of intestinal transit in the rat. J Pharmacol Methods 1981;6:211–7.
37. Penolazzi L, Lambertini E, Tavanti E, et al. Evaluation of chemokine and cytokine profiles in osteoblast progenitors from umbilical cord blood stem cells by BIO-PLEX technology. Cell Biol Int 2008;32:320–5.
38. Harting MT, Sloan LE, Jimenez F, Baumgartner J, Cox CS Jr. Subacute neural stem cell therapy for traumatic brain injury. J Surg Res 2009;153:188–94.